with stercomes or hollow) or the granellare was only present on one side of the polygon. However, other epifaunal syringamminid xenophyophores with polygonal anastomosing networks of tubes do have anastomosing granellare [for example, *Syringammina tasmanensis* (*4*)], and it is reasonable to suppose that in complete, living specimens the granellare of the present xenophyophore anastomose.

How or why the *Paleodictyon* organism maintains multiple vertical outlets has not been completely satisfactorily explained, but this can be understood in terms of a xenophyophore model: they could be outlets for the pseudopodia to gather food at the surface (Fig. 2B), and outlet separation may be determined by the "operation area" of the pseudopodia (that is, avoidance of overlap). The outlets may also act as "vents," providing the various branches of the organism's body with access to oxygenated sea water.

The abundance of dead sections suggests that the xenophyophore has to abandon sections of its network which have become filled with stercomare almost as fast as it can form them. Thus the gigantic and uniform size of some *Paleodictyon* nets (up to 1 m^2) (*9*) might be the result of a small threadlike organism (body width, ~ 100 μm or less) striving to maximize its areal coverage through netlike growth, while having to cope with a chronic waste disposal problem.

If *Paleodictyon* is a cast of a xenophyophore tube network, a question arises as to whether *Paleodictyon* is a trace fossil or a body fossil. Although the xenophyophore sediment tube is an order of magnitude larger in diameter than the unattached plasma body it encloses, it is nevertheless considered to be part of the organism, and its external shape is often characteristic at the species level (*4*). Thus, a cast of the tube system would seem to be a body fossil. However, the occurrence of the living organism at several centimeters depth in quite coherent sediment suggests that it may actively burrow, in which case the tube system could be regarded as a trace fossil. Alternatively, the organism may penetrate into the sediment like a root, rather than burrow.

In light of the proposed interpretation of *Paleodictyon*, the *Paleodictyon* grooves found on the tops of box cores by Ekdale (3) might be explained as either (i) the imprints of a xenophyophore tube system which had been lifted from the substrate and then fragmented by swilling sea water during or before drainage of the box core (as happened in this study), or (ii) part of the actual tunnel system of a dead xenophyophore in which the binding agent in the walls had decomposed (or was originally weak).

If *Paleodictyon* are traces of infaunal xenophyophores, the implications are quite far reaching. First, it would establish beyond doubt that *Paleodictyon* are reliable indicators of deep-sea sediments, since xenophyophores are almost exclusively restricted to the deep sea (*4*). Second, it would establish a history for xenophyophores extending back to Ordovician times; until now these primitive organisms have only been found in modern environments. Third, *Paleodictyon* would reflect an organism's growth, not its behavior. Lastly, the more than 30 ichnospecies of *Paleodictyon* (*9*) suggest the possible existence of many more species of infaunal xenophyophores, but care would have to be taken in their classification, as the presence of *Squamodictyon* within more angular *Paleodictyon* nets (*2*) indicates that morphological variation within a single species may be quite considerable.

D. D. Swinbanks
Ocean Research Institute,
University of Tokyo,
Tokyo 164, Japan

References and Notes

1. A. Seilacher, in *Trace Fossils 2*, T. P. Crimes and J. C. Harper, Eds. (Seel House, Liverpool, 1977), p. 289.
2. T. P. Crimes and J. D. Crossley, *J. Sediment. Petrol.* **50**, 821 (1980).
3. A. A. Ekdale, *Science* **207**, 304 (1980); P. A. Rona, *J. Geol. Soc. London* **137**, 385 (1980).
4. O. S. Tendal, in *Galathea Rep.* **12**, 1 (1972).
5. ——— and A. J. Gooday, *Oceanol. Acta* **4**, 415 (1981).
6. O. S. Tendal, D. D. Swinbanks, Y. Shirayama, *ibid.*, in press.
7. Determined by dry sieving down to 37 μm.
8. R. H. Hedley, appendix in K. B. Lewis, *N. Z. J. Sci.* **9**, 123 (1966).
9. W. Hantzschel, in *Treatise on Invertebrate Paleontology*, C. Teichert, Ed. (Univ. of Kansas Press, Lawrence, 1975), part W, suppl. 1, p. 1.
10. I thank the officers, crew, and scientists aboard R.V. *Hakuhō Maru* for their assistance in collecting box cores; P. Shinn for help in sample processing; S. Boggs, O. S. Tendal, and R. G. Bromley for reviewing the manuscript, and Y. Shirayama for first drawing my attention to an infaunal xenophyophore. Supported by a Monbusho Fellowship from the Japanese government.

23 March 1982; revised 30 June 1982

Crystal Site Location of Iron and Trace Elements in a Magnesium-Iron Olivine by a New Crystallographic Technique

Abstract. *A new crystallographic technique has been developed, which has been applied to the problem of locating the cations in a natural olivine crystal with the composition* $(Mg_{0.90}Fe_{0.10}Ni_{0.004}Mn_{0.002})_2SiO_4$. *The method uses the variation of characteristic x-ray emission with the direction of an exciting electron beam in an analytical transmission electron microscope. It may be applied to nanometer-sized areas and to concentrations as low as 0.1 atomic percent, is capable of distinguishing neighbors in the periodic table, and does not require external standards. The iron atoms in this crystal are evenly distributed between the two available crystal sites M1 and M2 (49.6 ± 1 percent on M1), whereas the trace elements nickel and manganese occupy the M1 and M2 positions, respectively (97 ± 5 percent nickel on M1 and 1 ± 5 percent manganese on M1).*

In many real crystals of interest to scientists, the three-dimensional periodic lattice of atomic sites is well defined. However, the assignment of particular species to these sites may be irregular, with resultant substitutional disorder. This determination of the distribution of atoms over available sites in crystals is of considerable interest in crystal chemistry, semiconductor physics, solid-state physics, and mineralogy; we deal here with a mineralogical problem. The degree of atomic order in a mineral serves as a geothermometer and geobarometer, giving petrologists information about the geologic and thermal history of rocks, such as the rate of cooling at the time of formation.

The most widely used methods for determining the positions of atoms in crystals are x-ray diffraction and neutron diffraction. However, difficulties arise when these techniques are applied to natural minerals as compared to laboratory-grown crystals, since, for a precise determination of the distribution of atoms in a crystal, the composition of the crystal must be known accurately. From the wealth of information that has been gathered over the last decade on the defect structure of minerals by transmission electron microscopy (*1*), it is now known that most natural minerals contain many inclusions of other phases. Thus the use of an average composition for x-ray structure analysis may obscure the chemical analysis of the crystal phase under study. This difficulty be-

Table 1. Results of the six different independent measurements showing the fraction C_X of Fe, Mn, and Ni on M1 sites.

Measurement	R(Si/Mg)	R(Si/Fe)	R(Si/Mn)	R(Si/Ni)	C_{Fe} (%)	C_{Mn} (%)	C_{Ni} (%)
1	1.64	1.59	1.02	3.17	47.0	2	111
2	1.93	1.89	1.04	4.10	48.3	2	99
3	1.45	1.48	0.98	2.12	52.2	−4	99
4	1.72	1.73	1.10	2.60	51.0	9	84
5	1.52	1.52	1.04	2.40	50.0	5	100
6	1.63	1.61	0.92	2.46	48.8	−9	89

comes crucial when one is dealing with small concentrations of atoms or when the atoms have similar scattering amplitudes, since an error in the assumed composition may influence the intensities of the Bragg reflections more than the presence of trace elements or small differences in scattering amplitudes.

Two important rock-forming minerals that may serve as petrogenic indicators are the pyroxenes and the olivines. In addition to O, Si, and Mg, these silicates may contain a large variety of first-row transition elements, often in small concentrations. In orthopyroxenes and olivines, Mg and the transition elements are distributed between two nonequivalent crystallographic positions denoted M1 and M2. However, because of the difficulties arising from the presence of other phases, only carefully selected minerals of high purity containing a small number of elements in crystal sites M1 and M2 (usually two elements, in high concentrations) have been studied by conventional diffraction techniques. By using an electron microscope, however, we are able to focus the electron beam down to a region a few nanometers in diameter if necessary so as to be able to analyze isolated microphases in natural minerals and we can avoid the use of artificially grown crystals.

We report here on the study of a yellow-green olivine from the San Carlos Indian Reservation, Arizona; the main element in the M1 and M2 positions is Mg, but in addition the crystal contains Fe and traces of Mn and Ni. The composition is approximately $(Mg_{0.90}Fe_{0.10}Ni_{0.004}Mn_{0.002})_2SiO_4$. The method used to locate the Mg, Fe, Ni, and Mn atoms is based on the dependence of the electron-induced x-ray emission from a thin crystal upon the crystallographic direction of the incident (100-keV) electron beam. This effect, known as the electron-channeling or Borrmann effect, has been studied for incident neutrons (*2*), x-rays (*3*), and electrons in another context (*4*). The incident electron establishes a periodic modulation across the unit cell. The characteristic x-ray emission excited by the electron beam is detected, and this is proportional to the magnitude of this electron wave field. One can vary the positions of the maxima in the wave field by changing the direction of the incident electron beam. We choose a "systematics" or "planar" channeling direction for the incident beam in which Bragg scattering from only one set of parallel crystal planes occurs. These planes are selected to separate the sites of interest into alternating nonequivalent planes.

Small crystal grains of olivine, obtained by grinding crystals in a mortar, were studied in an electron microscope (Philips 400T) equipped with an energy-dispersive x-ray analyzer (Tracor Northern) (energy resolution, 150 eV). A collimated beam of 100-keV electrons was used (divergence angle, 5 mrad) to illuminate 500-nm regions of crystal between 20 and 100 nm thick. Spectra were recorded over 500 to 1000 seconds at two orientations. The direction of the incident beam was chosen nearly parallel to the (010) planes for two reasons. First, the channeling effect is strong for this setting of the diffraction conditions, as can be seen if one compares the K_α line of Mn and Ni in Fig. 1. These two spectra (Fig. 1, a and b) are from the same crystal area. For Fig. 1a the angle between the incident beam and the (010) planes is slightly smaller than the Bragg angle for the first-order reflection, that is, the (020) reflection ($\theta_i < \theta_B$), and in Fig. 1b the crystal is tilted about 0.5° so that $\theta_i > \theta_B$. Second, the intensity of the wave field is the same on the Si atoms and the M2 sites, because they occupy the same plane in the projected structure (see the insets in Fig. 1). The x-ray emission from the Si atoms thus provides a reference signal proportional to the thickness-averaged intensity on the planes containing the M2 site. The approximate intensity of the modulated wave field is also shown in Fig. 1 (insets).

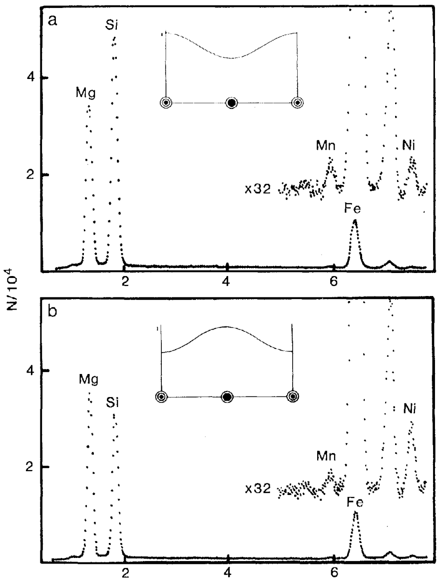

Fig. 1. X-ray emission spectra from the same area for two different incident beam directions: (a) $\theta_i < \theta_{020}$ and (b) $\theta_i > \theta_{020}$. Insets show the atomic arrangement along the (010) direction and an approximate calculation of the thickness-averaged electron intensity. The large (or outermost) circles in the insets are O, small (or innermost) circles Si, middle-sized open circles cations in the M2 site, and middle-sized, filled circles cations in the M1 site.

As a measure for the channeling effect we use

$$R(\mathrm{Si/X}) = [N_{Si}/N_X]_{\theta_i < \theta_B}/[N_{Si}/N_X]_{\theta_i > \theta_B} \quad (1)$$

where N_{Si} and N_X are, respectively, the K_α x-ray counts from Si and the element X (X = Mg, Mn, Fe, or Ni). Table 1 (first row) shows values of R(Si/X) obtained from background-subtracted peak areas integrated over a 70-eV window. The other rows in Table 1 show values of the same ratios from other independent measurements. The following general conclusions can be drawn from the results listed in Table 1. Since R(Si/Mn) is close to unity for all measurements, Mn is on the same plane as Si and therefore occupies the M2 site. Since R(Si/Fe) ≈ R(Si/Mg), Fe and Mg have about the same site preference. Since the concentration of trace elements is negligible and since there is an equal number of atoms on the M1 and M2 sites, it follows that very nearly 50 percent of the Fe and Mg atoms occupy each M site and this fraction is much closer to 50 percent for Mg because its concentration is ten times larger. Further, R(Si/Ni) > R(Si/Mg) shows that Ni has a preference for the M1 site.

From the fact that the Si atoms lie on the same planes as the M2 sites, it is possible to perform a quantitative analysis without calculating the intensity of the thickness-averaged electron wave field on the two types of planes. Generally for the olivine structure it is necessary to know the concentration of the major elements with reasonable accuracy, but in the present case, where we have already established that 50 percent of the Mg atoms occupy each M site, the analysis becomes particularly simple. The number of x-ray counts from any element Y in a spectrum is given by

$$N_Y = k_Y C_Y I_1 + k_Y(1 - C_Y)I_2 \quad (2)$$

where I_1 and I_2 are, respectively, the electron intensities on the M1 and M2 planes integrated over time and thickness, C_Y is the fraction of element Y on the M1 sites, and k_Y is a constant which depends on the efficiency of the spectrometer. From one spectrum taken under such conditions that the electron wave field is modulated ($I_1 \neq I_2$) and one with a uniform wave field ($I_1 = I_2$), the occupancy C_A for an element A can be shown to depend only on N_{Si}, N_{Mg}, and N_A as obtained from the two spectra. The analysis used to determine C_{Fe}, C_{Mn}, and C_{Ni} in Table 1 is essentially as described above. However, in order to improve the statistical accuracy, three spectra were used for each measurement. For two of the spectra the incident beam directions were as in Fig. 1, and for the third spectrum strong reflections were avoided so that $I_1 = I_2$ [see (*5*) for details]. Despite the variations in *R*(Si/Mg), *R*(Si/Fe), and *R*(Si/Ni), which result from slightly different experimental conditions of thickness and orientation, the site occupancies derived from these *R* values agree closely. From Table 1 we obtain $C_{Fe} = 49.6 \pm 1$ percent, $C_{Mn} = 1 \pm 5$ percent, and $C_{Ni} = 97 \pm 5$ percent.

Except for Fe, these site preferences agree with those predicted by Burns (*6*) for an Mg-olivine. It is, however, well known that theory fails to predict the Fe occupancy, and the surprising result that both Fe and Mg have similar site preferences between dissimilar sites has been confirmed in other experiments, such as that by Burns (*6*) on natural olivine with the use of optical absorption spectroscopy. Studies of synthetic and heat-treated Mg-Mn (*7*) and Mg-Ni (*8*) olivines show a much lower degree of ordering, an indication that the complete ordering of Mn and Ni found in our study is characteristic of a rock that is slowly cooled. The two main factors governing site preference in olivines are thought to be cation size and crystal field stabilization energy. For Fe, these factors are believed to compensate each other completely. It is known that Mn^{2+} experiences no crystal field effect, and the size of Mn^{2+} relative to Mg^{2+} indicates that the Mn atoms should occupy the larger M2 site. Since there is little size difference between Ni and Mg, Ni appears strongly influenced by crystal field effects. However, the prediction of cation site preferences is far from simple, and a large number of factors may influence the result (*9*).

Our results demonstrate that the orientation dependence of electron-induced characteristic x-ray emission can be used to determine quite accurately the cation distribution in olivine and also that of the trace elements. To our knowledge, no other single technique is capable of doing this for the small areas, low concentrations, and neighboring elements used in this study. Few assumptions have been made, the main one being that the localization of the various K_α processes is the same. A small systematic error may thus be introduced. However, the results of other workers (*10*) suggest that this effect is unlikely to affect C_X by more than 1 percent. For more complicated structures, dynamical calculations can be used in conjunction with quantitative analysis. It is expected that the method will be useful for the elucidation of many crystal structures in addition to the spinel, olivine, and sphalerite structures already studied (*5, 11*).

J. TAFTØ
J. C. H. SPENCE

Department of Physics,
Arizona State University,
Tempe 85287

References and Notes

1. H. R. Wenk, Ed., *Electron Microscopy in Mineralogy* (Springer-Verlag, New York, 1976).
2. J. W. Knowles, *Acta Crystallogr.* **9**, 61 (1956).
3. B. W. Batterman, *Phys. Rev. Sect. A* **133**, 759 (1964).
4. D. Cherns, A. Howie, M. H. Jacobs, *Z. Naturforsch Teil A* **28**, 565 (1973).
5. J. Taftø, *J. Appl. Crystallogr.*, **15**, 378 (1982).
6. R. G. Burns, *Am. Mineral.* **55**, 1608 (1970).
7. C. A. Francis and P. H. Ribbe, *ibid.* **65**, 1263 (1980).
8. V. Rajamani, G. E. Brown, C. T. Prewitt, *ibid.* **60**, 292 (1975).
9. D. L. Bish, *ibid.* **66**, 770 (1981).
10. A. J. Bourdillion, P. G. Self, W. M. Stobbs, *Philos. Mag. A* **44**, 1335 (1981).
11. J. Taftø and Z. Liliental, *J. Appl. Crystallogr.* **15**, 260 (1982); J. Taftø and J. C. H. Spence, *Ultramicroscopy*, in press.
12. We acknowledge the support provided by the staff of the NSF High-Resolution Electron Microscopy facility at Arizona State University and useful discussions with J. Smyth, M. O'Keeffe, and P. Buseck for the provision of specimens. This research was funded under NSF grant DMR8002108.

29 April 1982; revised 6 July 1982

Hydration Aging of Nuclear Waste Glass

Abstract. *The aging of simulated nuclear waste glass by contact with a controlled-temperature, humid atmosphere results in the formation of a double hydration layer penetrating into the glass and in the formation of minerals on the glass surface. The hydration process described here provides insight into the aging kinetics of naturally occurring glasses and also suggests that simulated aging reactions are necessary for demonstrating that nuclear waste forms can meet projected Nuclear Regulatory Commission requirements.*

Two facets of glass hydration are of current interest. The extent of surface hydration offers archeologists a method of dating prehistoric (*1, 2*) and more recent man-made (*3*) artifacts. The reverse process, the aging of simulated glass through induced hydration, can help to provide a sound, demonstrable technical basis for predicting the long-term performance of nuclear waste glass (*4*).

The hydrated layer (perlite) that forms on natural glasses has a higher water content (~ 3.5 percent by weight) than the bulk glass (~ 0.1 percent). This layer has been observed microscopically under polarized light and with either ^{15}N (*5*) or ^{19}F (*6*) nuclear resonance depth profiling. The hydrated layer forms by the exchange of mobile alkali metal ions from the bulk glass with protons, during which process the silicate network is believed to remain virtually unchanged (*7*). Tsong *et al.* have shown (*8*) that, in obsidian, surface hydration is accompanied by dealkalization and a buildup of calcium and magnesium in the outermost layers. The reaction kinetics ascribed to both field samples and simulated laboratory glasses were initially shown to follow a $t^{1/2}$ diffusion-type rate equation, where *t* is time (*1, 2*). However, other experimenters, using field samples, have had difficulty reproducing this rate law and report a time dependence ranging from $t^{1/3}$ to t^3 (*9*).

These disparate results have been attributed to an incomplete knowledge of weathering conditions and to less-than-rigorous segregation of glasses having different compositions. Clearly, composition, temperature, and water vapor concentration affect layer formation. It is possible that the differences between natural and simulated hydration cannot be reconciled (*10*), but certainly the dat-

0036-8075/82/1001-0051$01.00/0